

Dynamic Response Analysis of Sudden Enlargement and Sudden Contraction Pipe Conveying Fluid at Different End Conditions Using a Finite Element Method

Ali Mohammed Ridha Mahdi Al-Baheli

Maintenance Department of Fields Equipments and Wells Heads, Drilling and Work over Division, South Oil Company, Basrah, Iraq.

Abstract

Dynamic behavior of pipe conveying fluid at different cross section is investigated. Three kinds of supports are used, which are flexible, simply and rigid supports. The type effect of support on vibration characteristics and dynamic specification are studied. Also, the effect of some design parameters such as pipe material and Reynold numbers are investigated.

The governing equations of motion for this system are derived using the finite element method which depends on beam theory. A finite element software (ANSYS-11) is presented to find first three eigenvalue (natural frequency) and eigenvector (mode shape) for pipe system in modal analysis. Velocity and pressure distribution are evaluated in a single phase fluid flow. A coupled field fluid-structure analysis was then performed by transferring fluid forces, solid displacements, and velocity across the fluid-structure interface. Finally the effective stresses (Von mises stress) in piping system are predicted in static analysis at various Reynold numbers, pipe material and pipe supports.

تحليل الاستجابة الديناميكية لأنبوب ينقل مائع ذو توسع مفاجئ وتقلص مفاجئ وعند ظروف نهاية مختلفة باستخدام طريقة العناصر المحددة

علي محمد رضا مهدي الباهلي

قسم صيانة معدات الحقول ورؤوس الآبار، هيئة الحفر والاستصلاح
شركة نفط الجنوب، بصرة، العراق

الخلاصة

تم دراسة السلوك الديناميكي لأنبوب ينقل مائع. حيث تم استخدام ثلاثة أنواع من المساند متمثلة بالمسند المرن، المسند البسيط، والمسند الصلب. تم دراسة تأثير نوع المسند على خواص الاهتزاز والمواصفات الديناميكية للمنظومة. كما تم دراسة تأثير بعض المحددات مثل معدن الأنبوب ورقم رينولد. تم اشتقاق المعادلات الحاكمة للمنظومة باستخدام طريقة العناصر المحددة وبالاعتماد على نظرية (beam). استخدم (ANSYS-11 software) لإيجاد أول ثلاثة ترددات طبيعية وأول ثلاثة أشكال نسقيه للمنظومة بطريقة (modal analysis). تم تخمين توزيع السرعة والضغط لجريان المائع على طول الأنبوب. تم تحليل منطقة التداخل بين المائع والهيكِل وذلك بنقل القوة المسلطة من قبل المائع، إزاحة هيكِل الأنبوب، والسرعة عبر منطقة التداخل بين المائع والهيكِل. وأخيرا تم التنبؤ بالاجهادات المؤثرة (Von mises stress) في منظومة الأنابيب بطريقة (static analysis) وعند مختلف رقم رينولد، معدن الأنبوب ومساند الأنبوب.

Key words: Dynamic, Pipe Conveying Fluid, Finite Element Method, Fluid-Structure Interaction, Vibration.

Notations

ALE	Arbitrary Lagrangian Eulerian.	A_p	Cross-section area of the beam.
A_f	Cross-section area of the fluid.	E_p	Young's modules of elasticity.

F	Force.
F.E.M.	Finite element method.
[K]	Stiffness matrix.
M	Moment.
m_f	Mass density of the fluid.
m_p	Mass density of the beam.
P	Fluid pressure.
q	Fluid transverse distributed load along the length of the beam.
Q	Shear force.
Q_i	Element end contributions from the extensional terms.
\hat{Q}_I	Element end contributions from the bending terms.
r_i	Inlet radius.
r_0	Outlet radius.
Re	Reynold number.
t	Time.
u	Total displacement along the x-direction.
u_o, w_o	Axial and transverse displacements of a point on the natural axis.
V	Velocity of fluid.
w_o	Total displacement along the z-direction.
$\begin{bmatrix} \\ \end{bmatrix}$	Matrix.
$\begin{bmatrix} - \\ - \end{bmatrix}$	Vector.
δK	Virtual kinetic energy.
$\delta \Pi$	Virtual work in the beam.
δU	Virtual work due to internal forces.
δV	Virtual work due to external forces.
$\delta u_o, \delta w_o$	Virtual displacement.
ϵ_{xx}	Nonlinear strain-displacement.
Φ	Slop.
φ_i	Hermite cubic interpolation functions.
σ_r	Radial stress.
σ_t	Tangential stress.
ψ_j	Linear Lagrange interpolation function.
$\left(\frac{\partial w_o}{\partial x}\right)^2$	Rotation of transverse normal line in the beam.

Introduction

Several practical structures, in different engineering fields, are subjected to vibration as a result of the flow induced phenomena. Such behavior can compromise the integrity of the structure or make it uncomfortable for human use. The analysis of these problems involves the study of a coupled fluid-structure interaction model which can be accomplished using computational modeling. The numerical simulation of such applications is commonly performed using an interface approach involving the modification of the computational domain as the geometry under consideration is changing with time. In order to avoid updating the computational discretization too frequently, an Arbitrary Lagrangian Eulerian (ALE) formulation (Nomura and Hughes, [1]; Childs, [2]) is normally adopted together with a mesh movement algorithm. In such approach, generally the reference frame at the moving interface between the structure and the fluid has a Lagrangian description, and regions away from the interface have a mixed Lagrangian and Eulerian description to accommodate the arbitrary movement of the frame of reference.

In this paper, the finite element method is used to investigate the effect of the support types, pipe material and Reynold numbers for both sudden enlargement and construction pipe conveying fluid on the natural frequencies (eigenvalue), mode shapes (eigenvector) and stresses. To complete the problem a simplified approach is user. The fluid-structure system is subdivided into two subsystems, namely the structure domain and the fluid domain. By doing this, it is possible to deal with the following two separate problems:

- 1- The dynamic response of the structure to known loading.
- 2- The pressure generated in the fluid domain due to known motions of its boundaries.

The final step is to couple the solutions of those two problems along the interface boundary.

The analysis of such model application gives insight on many problems of industrial interest such as feed lines to sophisticated high performance rockets and aircrafts, reactors system components, water turbines, and heat exchangers.

Many researchers have been carried out on the dynamics of a pipe conveying fluid. Amabili, et. al. [3] investigated the non-linear dynamic and stability of simply supported circular cylindrical shells containing in-viscid incompressible fluid flow. Manabe, et. al. [4] discussed the dynamic stability of a flow conveying pipe with two lumped masses by using domain decomposition boundary element method. Amabili, et. al. [5] investigated the response of a shell conveying fluid to harmonic excitation, in the spectral neighborhood of one of the lowest natural frequencies for different flow velocities. Yih-Hwang and Chih-Liang [6] studied the vibration control of Timoshenko pipes conveying fluid. Excessive vibration in this flow induced vibration problem which was suppressed via an active feedback control scheme. Nawaf M. Bou-Rabee [7] examined the stability of a tubular cantilever conveying fluid in a multi-parameter space based on non-linear beam theory. Lee and Chung [8] presented a new non-linear model of a straight pipe conveying fluid for vibration analysis when the pipe is fixed at both ends. Using both the Euler-Bernoulli beam and the non-linear Lagrange strain theories, and from the extended Hamilton's principle, the coupled non-linear equations of motion for the longitudinal and transverse displacements are derived. These equations of motion are discretized by using the Galerkin method. Kuiper and Metrikine [9] proofed analytically the stability of a clamped-pinned pipe conveying fluid at a low speed. A tensioned Euler-Bernoulli beam in combination with a plug flow model was used as a model. The stability was studied employing a D-decomposition

method. Langre et. al. [10] considered the stability of a thin flexible cylinder which was regarded as a beam when subjected to axial flow and fixed at the upstream end only. A linear stability analysis of transverse motion aims at determining the risk of flutter as a function of the governing control parameters such as the flow velocity or the length of the cylinder. Stability is analyzed applying a finite difference scheme in space to the equation of motion expressed in the frequency domain.

Formulation of problem

1- Displacements and Strains

The Euler-Bernoulli hypothesis requires that plane sections as shows in fig. (1) perpendicular to the axis of the beam before deformation remains (a) plane, (b) rigid (not deform), and (c) rotate such that they remain perpendicular to the (deformed) axis after deformation [11].

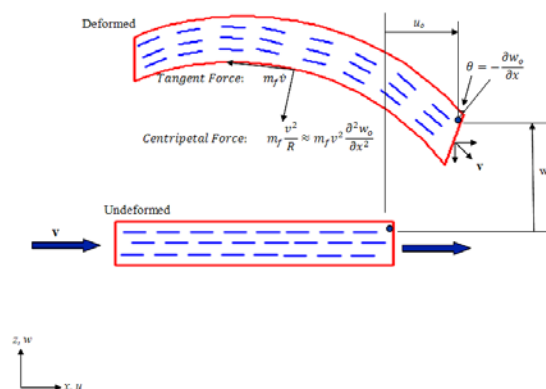


Fig. (1) An element of beam conveying fluid in the Euler-Bernoulli beam theory.

The assumptions are mounted to neglect both the Poisson effect and transverse strains. The bending of beams with moderately large rotations but with small strains can be derived using the following displacement field equations [12] :

$$u_{(x,z,t)} = u_o(x,t) - z \frac{\partial w_o}{\partial x} \dots\dots\dots(1)$$

$$w_{(x,z,t)} = w_o(x,t) \dots\dots\dots(2)$$

Using the nonlinear strain-displacement relations and by omitting the large strain terms but retaining only the square of $\partial w_o/\partial x$, the following equation could be obtained:

$$\begin{aligned} \epsilon_{xx} &= \frac{\partial u_o}{\partial x} + \frac{1}{2} \left(\frac{\partial w_o}{\partial x} \right)^2 + z \left(-\frac{\partial w_o}{\partial x^2} \right) \\ &= \epsilon_{xx}^0 + z\epsilon_{xx}^1 \dots\dots\dots(3) \end{aligned}$$

2- Virtual Work

Assume that the beam is hollow and is subjected to a transverse distributed load of $q_{(x,t)}$ along the length of the pipe, and suppose that a fluid with velocity $\mathbf{v}_{(t)}$ is being conveyed by the beam. The distributed load may include the weight of the beam as well as the fluid, and also the hydrostatic pressure if the beam is submerged in water. The forces on the beam due to the centripetal and tangential accelerations of the fluid can be accounted for in the potential energy of the loads as shown in Fig. 1. The fluid velocity $\mathbf{v}_{(t)}$ also contributes to the kinetic energy of the system. Since the primary interest is in deriving the equations of motion, the nature of the boundary conditions of the beam that experiences a displacement field of the form in Eqs. (1), (2).

The dynamic version of the principle of virtual displacements is given by [13] :

$$\int_0^T [\delta\Pi - \delta K] dt = 0 \dots\dots\dots(4)$$

$$\int_0^T [(\delta U - \delta V) - \delta K] dt = 0 \dots\dots\dots(5)$$

Where:

$$\delta U = \int_0^L \int_{A_p} \sigma_{xx} \left(\delta\epsilon_{xx}^{(0)} + z\delta\epsilon_{xx}^{(1)} \right) dA dx \dots\dots (6)$$

$$\delta V = \int_0^L \left[q\delta w_o - m_f v^2 \frac{\partial^2 w_o}{\partial x^2} (\sin\theta\delta u_o + \cos\theta\delta w_o) - m_f v (\cos\theta\delta u_o - \sin\theta\delta w_o) \right] dx \dots\dots (7)$$

$$\begin{aligned} \delta K &= \int_0^L \int_{A_p} \rho_p \left[\left(\dot{u}_o - z \frac{\partial \dot{w}_o}{\partial x} \right) \left(\delta \dot{u}_o - z \partial \delta w_o \partial x + w_o \delta w_o \right) dA dx + \right. \\ &\left. \int_0^L \int_{A_f} \rho_f \left[\mathbf{v} \cdot \delta \mathbf{v} + z^2 \left(\frac{\partial \dot{w}_o}{\partial x} \right) \left(\frac{\partial \delta \dot{w}_o}{\partial x} \right) \right] dx \dots(8) \right. \end{aligned}$$

And

$$\begin{aligned} \mathbf{v} &= (v \cos\theta + \dot{u}_o) \hat{\mathbf{i}} \\ &\quad + (-v \sin\theta + \dot{w}_o) \hat{\mathbf{j}}, \\ \theta &= -\frac{\partial w_o}{\partial x} \dots\dots\dots(9) \end{aligned}$$

3- Euler—Lagrange Equations

Substituting for $\delta\Pi$ and δK from Eqs. (6), (7), and (8) into Eq. (5), the following equation could be obtained [13] :

$$\begin{aligned} 0 &= \int_0^T \int_0^L \left\{ N_{xx} \delta\epsilon_{xx}^{(0)} + M_{xx} \delta\epsilon_{xx}^{(1)} - m_p u_o \delta u_o + w_o \delta w_o - I_p + I_f \partial w_o \partial x \partial \delta w_o \partial x - m_f v \cos\theta \right. \\ &\quad \left. + u_o \delta v \cos\theta + u_o + v \sin\theta - w_o \delta v \sin\theta - w_o \right\} dx dt \\ &\quad - \int_0^T \int_0^L \left[q \delta w_o - m_f v^2 \frac{\partial^2 w_o}{\partial x^2} (\sin\theta \delta u_o + \cos\theta \delta w_o) - m_f v \cos\theta \delta u_o - \sin\theta \delta w_o \right] dx dt \dots\dots\dots(10) \end{aligned}$$

$$= \int_0^T \int_0^L \left[-\frac{\partial N_{xx}}{\partial x} + (m_p + m_f) \frac{\partial^2 u_o}{\partial t^2} + m_f v \sin\theta \partial^2 w_o \partial x \partial t + v \partial^2 w_o \partial x^2 + m_f v \cos\theta \delta u_o \right] dx dt$$

$$\begin{aligned} &+ \int_0^T \int_0^L \left\{ -\frac{\partial^2 M_{xx}}{\partial x^2} - \frac{\partial}{\partial x} \left(\frac{\partial w_o}{\partial x} N_{xx} \right) + (m_p + m_f) \frac{\partial^2 w_o}{\partial t^2} - (\hat{I}_p + \hat{I}_f) \frac{\partial^4 w_o}{\partial x^2 \partial t^2} - q \right. \\ &\quad \left. + m_f v^2 \cos\theta \frac{\partial^2 w_o}{\partial x^2} - m_f \dot{v} \sin\theta + m_f v \left[\cos\theta \left(2 \frac{\partial^2 w_o}{\partial x \partial t} - \frac{\partial u_o}{\partial t} \frac{\partial^2 w_o}{\partial x^2} \right) + \sin\theta \left(\frac{\partial^2 u_o}{\partial x \partial t} + \frac{\partial w_o}{\partial t} \frac{\partial^2 w_o}{\partial x^2} \right) \right] \right\} \delta w_o dx dt + \\ &\quad \int_0^T \left\{ N_{xx} \delta u_o - M_{xx} \frac{\partial \delta w_o}{\partial x} + \left[\frac{\partial M_{xx}}{\partial x} + \frac{\partial w_o}{\partial x} N_{xx} - (\hat{I}_p + \hat{I}_f) \frac{\partial^3 w_o}{\partial x \partial t^2} - m_f v (\sin\theta \dot{u}_o + \cos\theta \dot{w}_o) \right] \delta w_o \right\} L dt \dots\dots\dots(11) \end{aligned}$$

Where all the terms involving $[\dots]_0^T$ vanish on the assumption that all variations and their derivatives are zero at $t = 0$ and $t = T$. The variables introduced in arriving at the last expression are defined as follows:

$$\begin{aligned} \left\{ \begin{matrix} N_{xx} \\ M_{xx} \end{matrix} \right\} &= \int_{A_p} \left\{ \begin{matrix} 1 \\ z \end{matrix} \right\} \sigma_{xx} dA \\ m_p &= \int_{A_p} \rho_p dA = \rho_p A_p \\ m_f &= \int_{A_f} \rho_f dA = \rho_f A_f \\ \hat{I}_p &= \int_{A_p} \rho_p z^2 dA = \rho_p I_p \\ \hat{I}_f &= \int_{A_f} \rho_f z^2 dA = \rho_f I_f \end{aligned}$$

Thus, the Euler—Lagrange equations of motion are:

$$-\frac{\partial N_{xx}}{\partial x} + (m_p + m_f) \frac{\partial^2 u_o}{\partial t^2} + m_f v \sin\theta \left(\frac{\partial^2 w_o}{\partial x \partial t} + v \frac{\partial^2 w_o}{\partial x^2} \right) + m_f \dot{v} \cos\theta = 0 \quad \dots\dots(12)$$

$$-\frac{\partial^2 M_{xx}}{\partial x^2} - \frac{\partial}{\partial x} \left(\frac{\partial w_o}{\partial x} N_{xx} \right) + (m_p + m_f) \frac{\partial^2 w_o}{\partial t^2} - I_p \frac{\partial^4 w_o}{\partial x^2 \partial t^2} + I_f \frac{\partial^4 w_o}{\partial x^2 \partial t^2} + m_f v \left[\cos\theta \left(2 \frac{\partial^2 w_o}{\partial x \partial t} - \frac{\partial u_o}{\partial t} \frac{\partial^2 w_o}{\partial x^2} \right) + \sin\theta \frac{\partial^2 u_o}{\partial x^2} - m_f \dot{v} \sin\theta \right] = q \quad \dots\dots(13)$$

Equations (12) and (13) represent coupled nonlinear equations among (u_o, w_o) .

4- Finite element models

The finite element model of the equations of motion (12) and (13) can be constructed using the virtual work statement in Eq. (10). The virtual work statement over a typical element (x_a, x_b) can be written as follows [14]:

$$\begin{aligned} 0 &= \int_0^T \int_{x_a}^{x_b} \left\{ E_p A_p \left[\frac{\partial u_o}{\partial x} + \frac{1}{2} \left(\frac{\partial w_o}{\partial x} \right)^2 \right] \right. \\ &\quad \left. \left(\frac{\partial \delta u_o}{\partial x} + \frac{\partial w_o}{\partial x} \frac{\partial \delta w_o}{\partial x} \right) + E_p I_p \frac{\partial^2 w_o}{\partial x^2} \frac{\partial^2 \delta w_o}{\partial x^2} - (m_p + m_f) \right. \\ &\quad \left. (\dot{u}_o \delta \dot{u}_o + \dot{w}_o \delta \dot{w}_o) - (\hat{I}_p + \hat{I}_f) \frac{\partial \dot{w}_o}{\partial x} \frac{\partial \delta \dot{w}_o}{\partial x} - m_f v [\cos\theta \delta \dot{u}_o - \right. \\ &\quad \left. u_o \sin\theta + w_o \cos\theta \delta \theta - \sin\theta \delta w_o - q \delta w_o \right. \\ &\quad \left. + m_f v^2 \frac{\partial^2 w_o}{\partial x^2} (\sin\theta \delta u_o + \cos\theta \delta w_o) + m_f \dot{v} (\cos\theta \delta u_o - \right. \\ &\quad \left. \sin\theta \delta w_o) \right\} dx dt \quad \dots\dots\dots(14) \end{aligned}$$

which is equivalent to the following two statements:

$$\begin{aligned} 0 &= \int_0^T \int_{x_a}^{x_b} \left\{ E_p A_p \left[\frac{\partial u_o}{\partial x} + \frac{1}{2} \left(\frac{\partial w_o}{\partial x} \right)^2 \right] \frac{\partial \delta u_o}{\partial x} + \right. \\ &\quad \left. (m_p + m_f) \ddot{u}_o \delta u_o + m_f v \sin\theta \left(\frac{\partial^2 w_o}{\partial x \partial t} + v \frac{\partial^2 w_o}{\partial x^2} \right) \delta u_o + \right. \\ &\quad \left. m_f \dot{v} \cos\theta \delta u_o \right\} dx dt \quad \dots\dots\dots(15) \end{aligned}$$

$$\begin{aligned} 0 &= \int_0^T \int_{x_a}^{x_b} \left\{ E_p A_p \left[\frac{\partial u_o}{\partial x} + \frac{1}{2} \left(\frac{\partial w_o}{\partial x} \right)^2 \right] \frac{\partial w_o}{\partial x} \frac{\partial \delta w_o}{\partial x} \right. \\ &\quad \left. E_p I_p \frac{\partial^2 w_o}{\partial x^2} \frac{\partial^2 \delta w_o}{\partial x^2} \right\} dx dt + (m_p + m_f) \ddot{w}_o \delta w_o \\ &\quad + (\hat{I}_p + \hat{I}_f) \frac{\partial \dot{w}_o}{\partial x} \frac{\partial \delta \dot{w}_o}{\partial x} + m_f v \left[-(\dot{u}_o \sin\theta + \right. \\ &\quad \left. \dot{w}_o \cos\theta) \frac{\partial \delta w_o}{\partial x} + \cos\theta \frac{\partial^2 w_o}{\partial x \partial t} \delta w_o \right] + \\ &\quad \left. m_f v^2 \frac{\partial^2 w_o}{\partial x^2} \cos\theta \delta w_o - m_f \dot{v} \sin\theta \delta w_o - \right. \\ &\quad \left. q \delta w_o \right\} dx dt \quad \dots\dots\dots(16) \end{aligned}$$

From fig. (2) the finite element approximations of the form [15] could be assumed as follows:

$$u_o(x,t) = \sum_{j=1}^2 u_j(t) \psi_j(x) \quad \dots\dots\dots(17)$$

$$w_o(x,t) = \sum_{j=1}^4 \bar{\Delta}_j(t) \varphi_j(x) \quad \dots\dots\dots(18)$$

$$\left. \begin{aligned} \bar{\Delta}_1(t) &\equiv w_o(x_a,t) \\ \bar{\Delta}_2(t) &\equiv -\theta(x_a,t) \\ \bar{\Delta}_3(t) &\equiv w_o(x_b,t) \\ \bar{\Delta}_4(t) &\equiv -\theta(x_b,t) \end{aligned} \right\} \dots\dots(19)$$

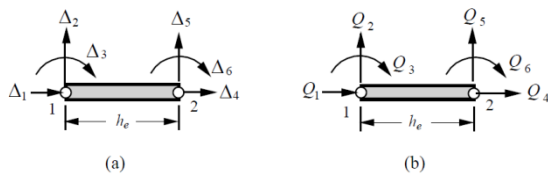


Fig. (2) A typical beam finite element with displacement and force degrees of freedom.

Substituting Eq. (19) for $u_o(x,t)$ and $w_o(x,t)$, and $\delta u_o(x) = \psi_i(x)$ and $\delta w_o(x) = \varphi_i(x)$ into the weak forms (16), (17) and (18), we obtain:

$$\begin{bmatrix} M^{11} & 0 \\ 0 & M^{22} \end{bmatrix} \begin{Bmatrix} \bar{\Delta}^1 \\ \bar{\Delta}^2 \end{Bmatrix} + \begin{bmatrix} 0 & C^{12} \\ C^{21} & C^{22} \end{bmatrix} \begin{Bmatrix} \bar{\Delta}^1 \\ \bar{\Delta}^2 \end{Bmatrix} + \begin{bmatrix} K^{11} & K^{12} \\ K^{21} & K^{22} \end{bmatrix} \begin{Bmatrix} \Delta^1 \\ \Delta^2 \end{Bmatrix} = \begin{Bmatrix} F^1 \\ F^2 \end{Bmatrix} \dots\dots\dots(20)$$

Where:

$$\Delta_i^1 = u_i, \quad \Delta_i^2 = \bar{\Delta}_i$$

for $i = 1,2$ and $I = 1, 2, 3, 4$. The element coefficients are :

$$M_{ij}^{11} = \int_{x_a}^{x_b} (m_p + m_f) \psi_i \psi_j dx$$

$$M_{ij}^{22} = \int_{x_a}^{x_b} [(m_p + m_f) \varphi_I \varphi_J + I p + I f d\varphi_I dx d\varphi_J dx dx$$

$$C_{ij}^{12} = \int_{x_a}^{x_b} m_f v \sin\theta \psi_i \frac{d\varphi_J}{dx} dx \approx - \int_{x_a}^{x_b} m_f v \frac{\partial w_o}{\partial x} \psi_i \frac{d\varphi_J}{dx} dx$$

$$C_{ij}^{21} = - \int_{x_a}^{x_b} m_f v \sin\theta \psi_j \frac{d\varphi_I}{dx} dx \approx \int_{x_a}^{x_b} m_f v \frac{\partial w_o}{\partial x} \psi_j \frac{d\varphi_I}{dx} dx$$

$$K_{ij}^{22} = - \int_{x_a}^{x_b} m_f v \cos\theta \left(\frac{d\varphi_J}{dx} \varphi_I - d\varphi_I dx \varphi_J \right) dx \approx \int_{x_a}^{x_b} m_f v \left(\frac{d\varphi_J}{dx} \varphi_I - \frac{d\varphi_I}{dx} \varphi_J \right) dx$$

$$K_{ij}^{11} = \int_{x_a}^{x_b} E_p A_p \frac{d\psi_i}{dx} \frac{d\psi_j}{dx} dx$$

$$K_{ij}^{12} = \frac{1}{2} \int_{x_a}^{x_b} \left[\left(E_p A_p \frac{\partial w_o}{\partial x} \right) \frac{d\psi_i}{dx} \frac{d\psi_j}{dx} + m_f v 2 \sin\theta \psi_i \frac{\partial^2 \varphi_J}{\partial x^2} \right] dx$$

$$\approx \frac{1}{2} \int_{x_a}^{x_b} \left[\left(E_p A_p \frac{\partial w_o}{\partial x} \right) \frac{d\psi_i}{dx} \frac{d\psi_j}{dx} + m_f v 2 \frac{\partial w_o}{\partial x} \frac{\partial^2 \varphi_J}{\partial x^2} \right] dx$$

$$K_{ij}^{21} = \int_{x_a}^{x_b} E_p A_p \frac{\partial w_o}{\partial x} \frac{d\varphi_I}{dx} \frac{d\psi_j}{dx} dx,$$

$$K_{ij}^{21} = 2K_{ij}^{12}$$

$$K_{ij}^{22} = \int_{x_a}^{x_b} E_p I_p \frac{\partial^2 \varphi_I}{\partial x^2} \frac{\partial^2 \varphi_J}{\partial x^2} dx +$$

$$12 x a x b E_p A_p \frac{\partial w_o}{\partial x} \frac{\partial^2 \varphi_I}{\partial x^2} \frac{d\varphi_J}{dx} dx dx + \int_{x_a}^{x_b} m_f v^2 \cos\theta \varphi_I \frac{\partial^2 \varphi_J}{\partial x^2} dx$$

$$\approx \int_{x_a}^{x_b} E_p I_p \frac{\partial^2 \varphi_I}{\partial x^2} \frac{\partial^2 \varphi_J}{\partial x^2} dx + \frac{1}{2} \int_{x_a}^{x_b} \left[E_p A_p \left(\frac{\partial w_o}{\partial x} \right)^2 \right] \frac{d\varphi_I}{dx} \frac{d\varphi_J}{dx} dx$$

$$- \int_{x_a}^{x_b} m_f v^2 \frac{d\varphi_I}{dx} \frac{d\varphi_J}{dx} dx + \int_{x_a}^{x_b} m_f v \frac{d\varphi_J}{dx} \varphi_I dx$$

$$F_i^1 = - \int_{x_a}^{x_b} m_f v \cos\theta \psi_i dx + Q_i \approx - \int_{x_a}^{x_b} m_f v \psi_i dx + Q_i$$

$$F_i^2 = \int_{x_a}^{x_b} q \varphi_I dx - \int_{x_a}^{x_b} m_f v \sin\theta \varphi_I dx + \hat{Q}_i$$

$$\approx \int_{x_a}^{x_b} q \varphi_I dx - \int_{x_a}^{x_b} m_f v \frac{\partial w_o}{\partial x} \varphi_I dx + \hat{Q}_i$$

Note that the coefficient matrices $[K_{12}]$, $[K_{21}]$ and $[K_{22}]$ are functions of the unknown $w_o(x, t)$. Stiffness coefficients are also given for the case in which $\cos\theta$ and $\sin\theta$ are approximated as $\cos\theta \approx 1$ and $\sin\theta \approx \theta$.

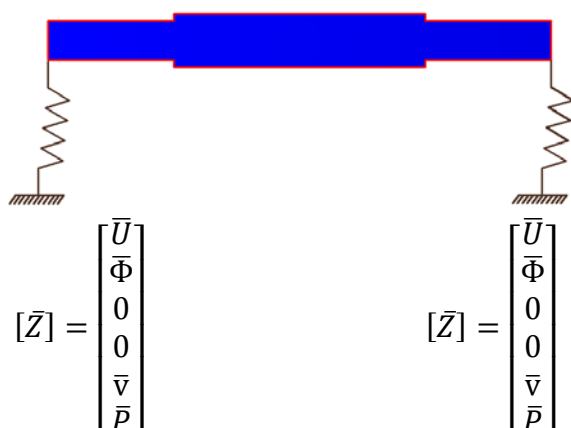
Boundary conditions

The boundary conditions give the descriptions of the state vector parameters at the supported ends of the pipe. To fully describe the situation at each node, four quantities must be known. These are the deflection (U), the slope (Φ), the moment (M), and the shear forces (Q). The present study added two fluid physical properties, which are velocity (v), and pressure (p) corresponding to the compressive and Coriolis forces due to flow induced vibration. These six quantities can be arranged in a vector as follows [16]:

$$[\bar{Z}] = \begin{bmatrix} \bar{U} \\ \bar{\Phi} \\ \bar{M} \\ \bar{Q} \\ \bar{v} \\ \bar{p} \end{bmatrix}$$

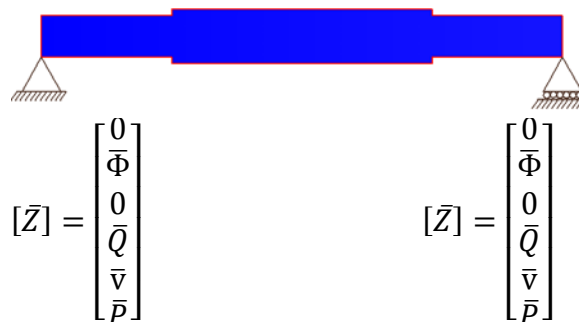
1- Flexible supports

For flexible supported case (with $K=11.86E4 \text{ N/m}^2$ for both sides [17]), the moment and the shear forces are equal to zero, and all other parameters have a value more than zero as shown below:



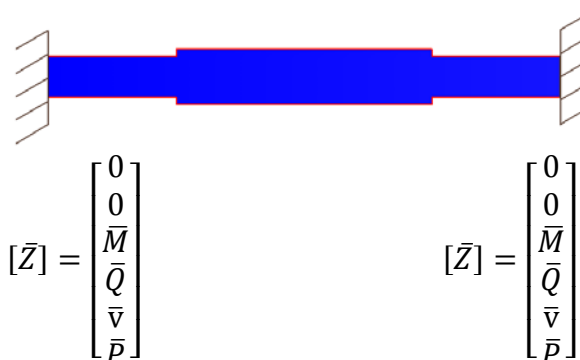
2- Simply supports

The deflection and the moment are both equal to zero in simply supported pipe ends, while the other parameters are not equal to zero as shown below:



3- Rigid supports

For rigid supports case, both the deflection and the slope are equal to zero, while the other parameters have a value greater than zero as shown below:



Finite element modeling procedure

The FE analysis was carried out to estimate the dynamic performance of pipes conveying fluid with different Reynold numbers and boundary conditions. This is accomplished by using a general purpose FE package (ANSYS V-11). The approach is divided into three parts: modal analysis, computational fluid dynamics (CFD), and coupled field fluid-structure analysis.

The Solid72 (3-dimension, tetrahedral element, four nodes, and six degree of freedom) is used to mesh the pipe and control on mesh by given element size, as shown in figure (3), while the fluid flow in pipe is represented in ANSYS-11 by using Fluid142 elements. The input for the solver is the velocity, while the output is the pressure. The pressure value is multiplied by the inside area of the pipe to obtain the force that applies the load on this system.

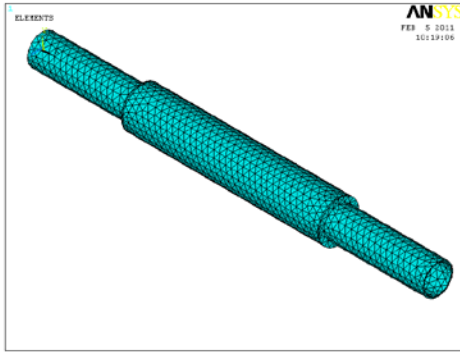


Fig. (3) Pipe mesh.

Modal analysis

Modal analysis is used to determine the vibration characteristics (natural frequencies and mode shapes) of pipe conveying fluid. The natural frequencies and mode shapes are important parameters in the design of a structure for dynamic loading conditions. The current reported results are the first three of the copper and steel pipes natural frequencies (eigenvalues) and mode shapes (eigenvectors) as shown in figs. (4), (5), (6), (7), (8) and (9).

The values of the natural frequencies for copper and steel pipes with flexible support are less than those for simply support by (37.933 % and 41.37 %) respectively and rigid support by (49.072 % and 45.6 %) respectively. Also, the values of natural frequencies for simply support are less than that for rigid support by (19.349 %) for copper pipe and by (22.883 %) for steel pipe. This is because the flexible support has the ability to move in y-direction. Therefore, its flexibility is very high comparing with both simply and rigid supports. The eigenvalues in steel pipe material are higher rather than the eigenvalues in copper pipe material. This is because of the modulus of rigidity is high in steel pipe (80-100 GN/m²), but for copper pipe the modulus of rigidity is (30-50 GN/m²) which is given more flexibility.

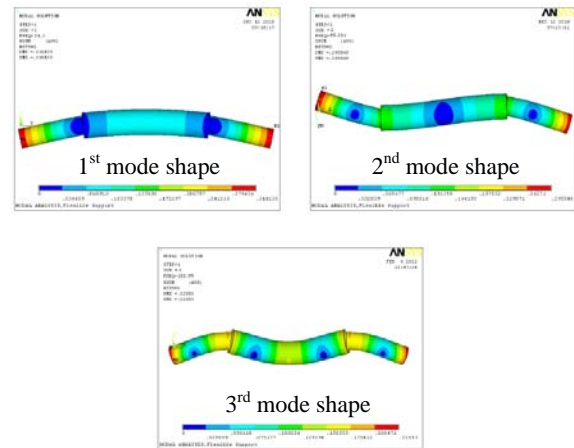


Fig. (4) Natural frequency and mode shape for copper pipe with flexible support.

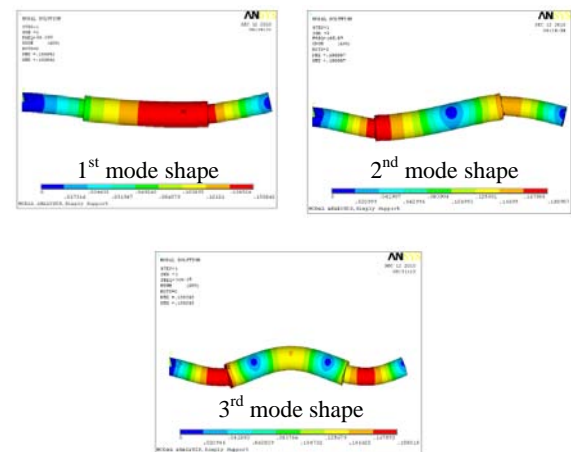


Fig. (5) Natural frequency and mode shape for copper pipe with simply support.

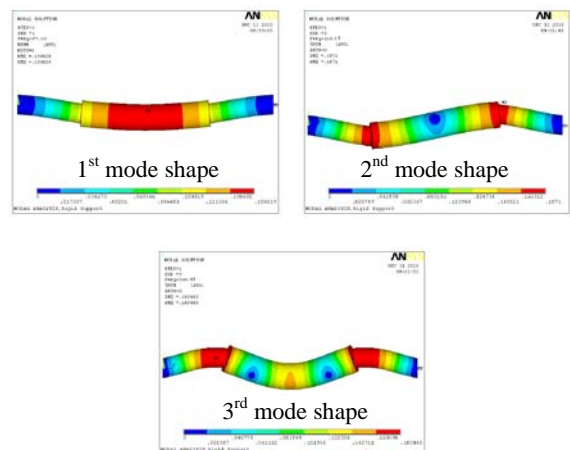


Fig. (6) Natural frequency and mode shape for copper pipe with rigid support.

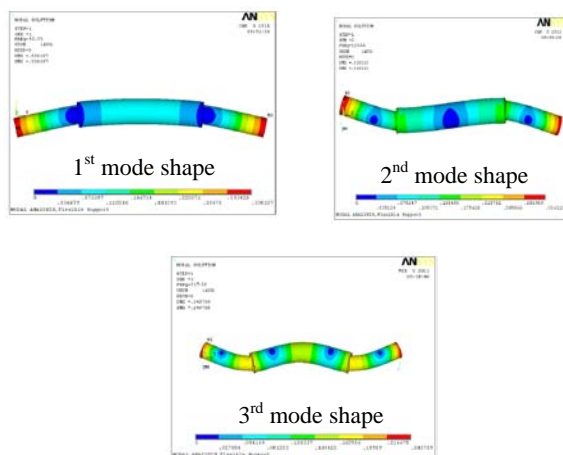


Fig. (7) Natural frequency and mode shape for steel pipe with flexible support.

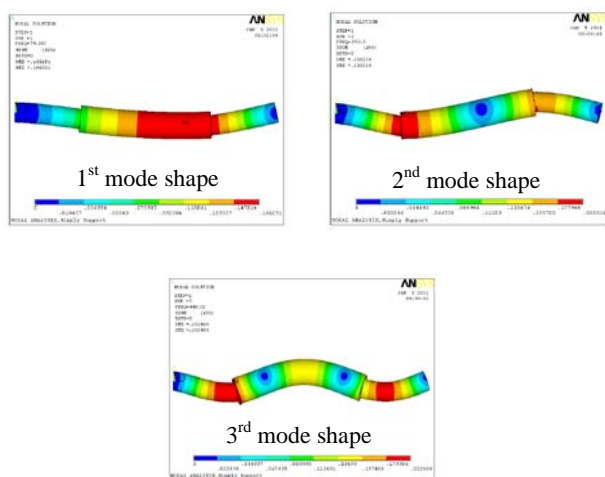


Fig. (8) Natural frequency and mode shape for steel pipe with simply support.

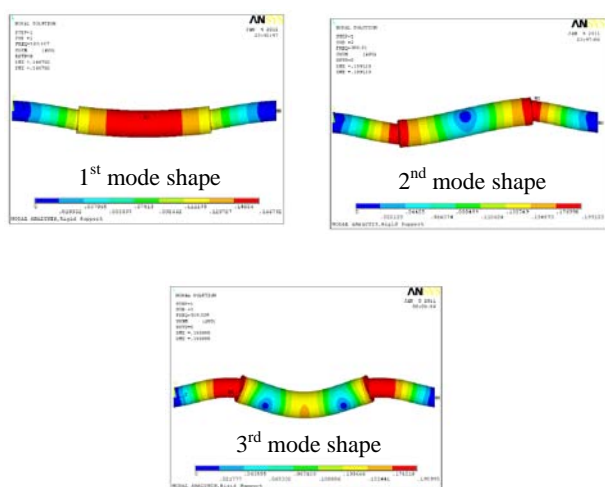


Fig. (9) Natural frequency and mode shape for steel pipe with rigid support.

Computational fluid dynamics (CFD)

The ANSYS flotran analysis used to solve the 3-D flow and pressure distributions in a single phase viscous fluid [18]. The velocities are obtained from the conservation of momentum principle, while the pressure is obtained from the conservation of mass principle. A segregated sequential solver algorithm is used; that is, the matrix system derived from the finite element discretization of the governing equation for each degree of freedom is solved separately. The flow problem is nonlinear and the governing equations are coupled together. The sequential solution of all the governing equations, combined with the update of any pressure dependent properties, constitutes a global iteration. The number of global iterations required to achieve a converged solution may vary considerably, depending on the size and stability of the problem .

The fluid pressure distribution along the pipe is predict in figure (10) at the different Reynold numbers. The pressure force was increased by (74.996 %) when the Reynold numbers varied from (500-1000), while the pressure force was increased by (55.55 %) when the Reynold numbers varied from (1000-1500). This is because of increased inertia force of fluid flow. Pressure force is appeared to have a maximum value at the pipe wall due to the effect of shear layer growth. So the velocity of fluid flow at the pipe wall is equal zero.

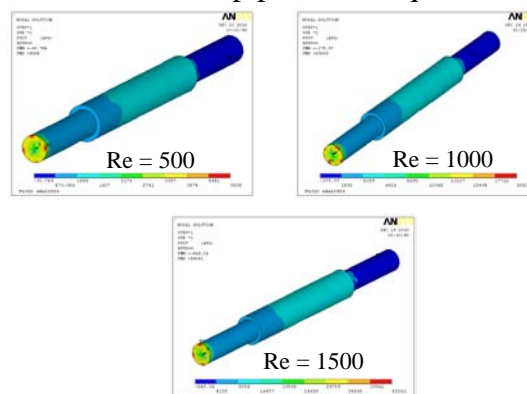


Fig. (10) Fluid pressure distribution along the pipe at different Reynold numbers.

The pressure force value of fluid flow is gradually reduced from the pipe wall down to the center of the pipe. This is due to increase in velocity of the fluid flow reaching to maximum value at the center of pipe as shown in fig. (11). Velocity of fluid flow was increased by (50 %) when the Reynold numbers varied from (500-1000), while velocity of fluid flow was increased by (33.33 %) when the Reynold numbers varied from (1000-1500).

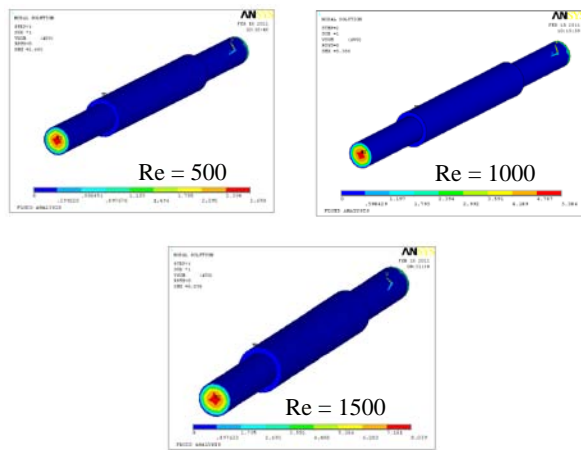


Fig. (11) Velocity of fluid distribution along the pipe at different Reynold numbers.

Figure (12) shows the velocity of fluid distribution at the outlet of the pipe section at different Reynold numbers and it can be seen that the velocity distribution is clearly to be fully developed flow.

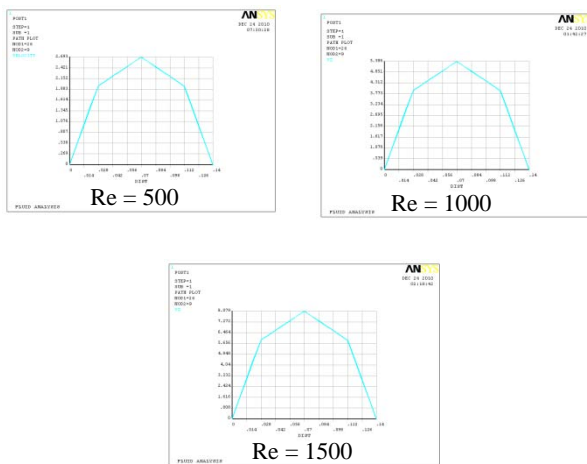


Fig. (12) Velocity of fluid distribution at the outlet of the pipe section at different Reynold numbers.

Coupled field fluid-structure analysis

Monolithic methods were approached to solve the fluid-structure interaction problem[19]. In this method, the discretized fluid-structure system is solved together with the mesh movement system in a single iteration loop. This will lead to a very large system of nonlinear equations to be solved simultaneously. Some advantages of this method are to ensure stability and convergence of the whole coupled problem. On the contrary, in simultaneous solution procedures, the time step has to be equal for all subsystems. This may be inefficient if different time scales are presented for the problem. An important disadvantage is the considerable high computing time effort required to solve each algebraic system and sometimes the necessity to develop a new software and solution methods for the coupling method.

Static analysis of fluid-structure interaction

A static analysis calculates the effects of steady loading conditions on a structure, while ignoring inertia and damping effects, such as those caused by time-varying loads [20]. Static analysis determines the displacements, stresses, strains, and forces in structures or components caused by loads.

The stresses in pipes due to the internal fluid pressure are determined by lame's equation (tangential stress and radial stress) at any radius x [21].

$$\sigma_t = \frac{p(r_i)^2}{(r_o)^2 - (r_i)^2} \left[1 + \frac{(r_o)^2}{x^2} \right] \dots\dots\dots(21)$$

$$\sigma_r = \frac{p(r_i)^2}{(r_o)^2 - (r_i)^2} \left[1 - \frac{(r_o)^2}{x^2} \right] \dots\dots\dots(22)$$

The tangential stress is maximum at the inner surface (when $x=r_i$) of the pipe and minimum at the outer surface (when $x=r_o$) of the pipe.

The radial stress is maximum at the inner surface (when $x=r_i$) of the pipe and

zero at the outer surface (when $x=r_o$) of the pipe.

Figures (13),(14), (15),(16), (17), and (18) depict the contour stress distribution along the copper and steel pipes at different Reynold numbers, and pipe supports. It can be seen that the stress value in copper and steel pipes increased by (74.99 %) when the Reynold numbers varied from (500-1000), while the stress value increased by (55.55 %) when the Reynold numbers varied from (1000-1500). This increased refer to increase inertia force of fluid flow which lead to increase fluid pressure.

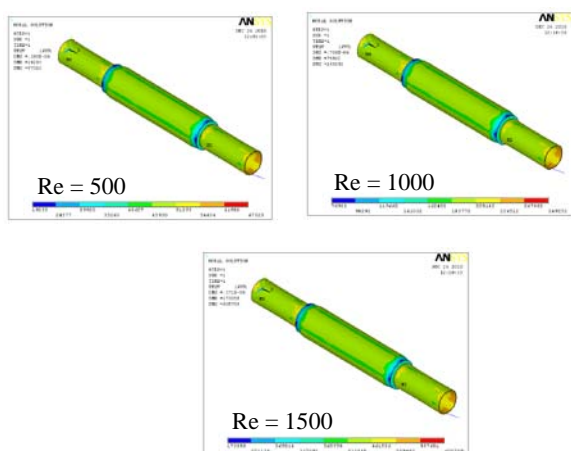


Fig. (13) Stress distribution along the copper pipe with Flexible support.

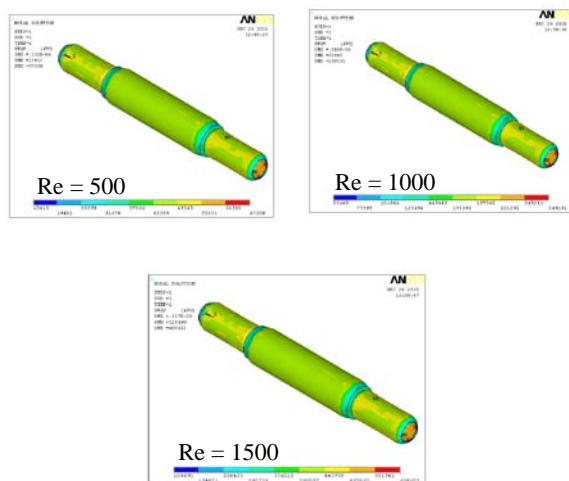


Fig. (14) Stress distribution along the copper pipe with Simply support.

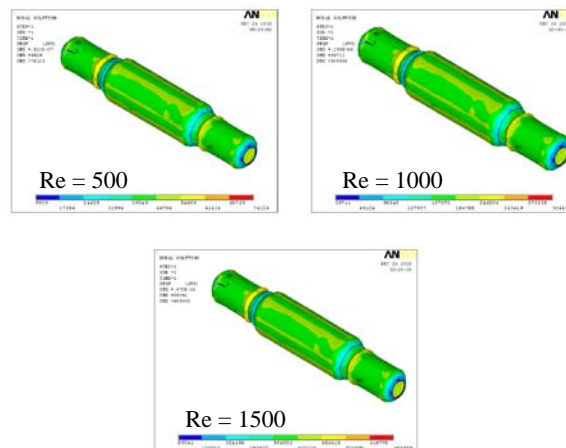


Fig. (15) Stress distribution along the copper pipe with Rigid support.

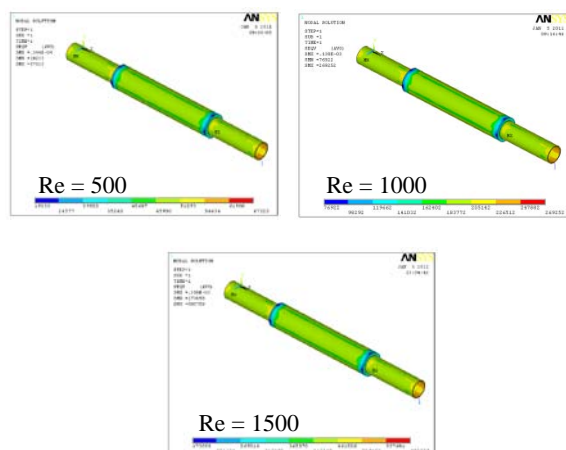


Fig. (16) Stress distribution along the steel pipe with Flexible support.

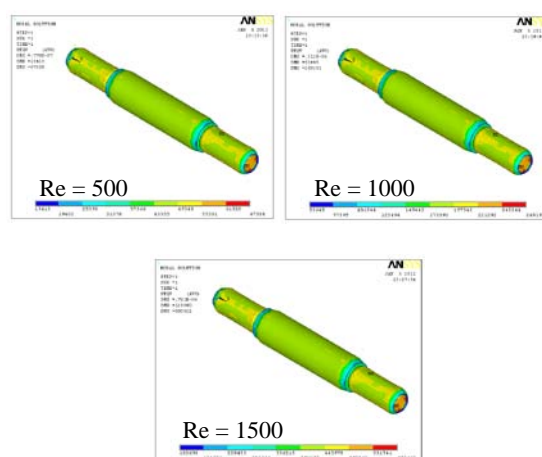


Fig. (17) Stress distribution along the steel pipe with Simply support.

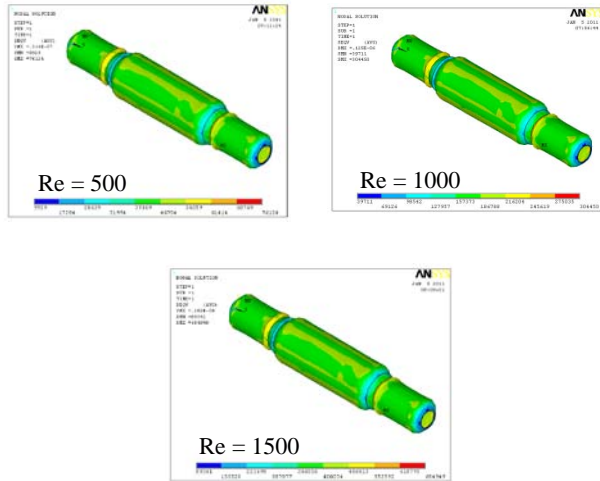


Fig. (18) Stress distribution along the steel pipe with Rigid support.

The stress in small pipe diameter is high than the stress in large pipe diameter. This is because to reduce cross section area in small pipe diameter which is reverse proportional with stress. In sudden contraction region, the liquid flows from large pipe diameter to small pipe diameter, the area of flow goes on decreasing and becomes minimum at this section. After this suction a sudden enlargement of the area takes place [22]. The loss of head due to sudden contraction is reduced the stress as shown in Figures (19), (20), (21), (22), (23) and (24).

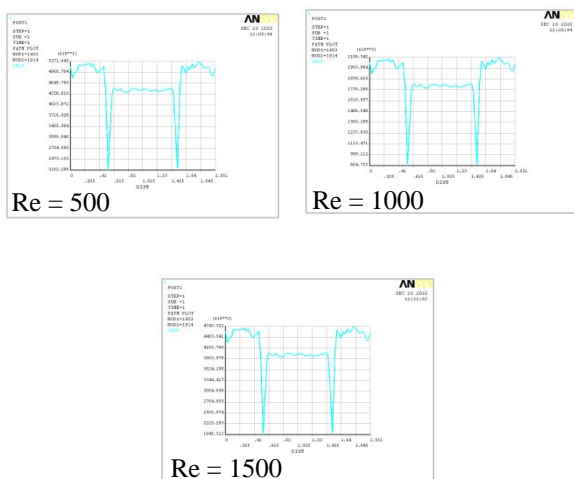


Fig. (19) Von Mises stress distribution along the copper pipe with Flexible support.

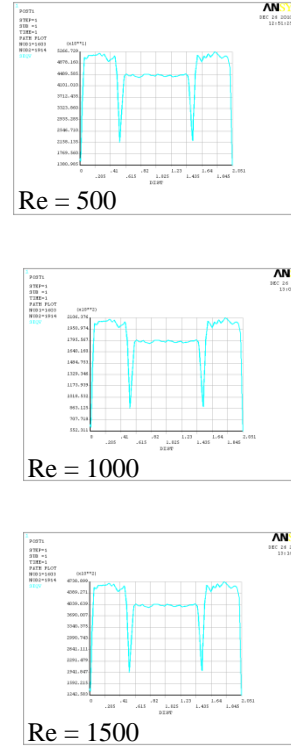


Fig. (20) Von Mises stress distribution along the copper pipe with Simply support.

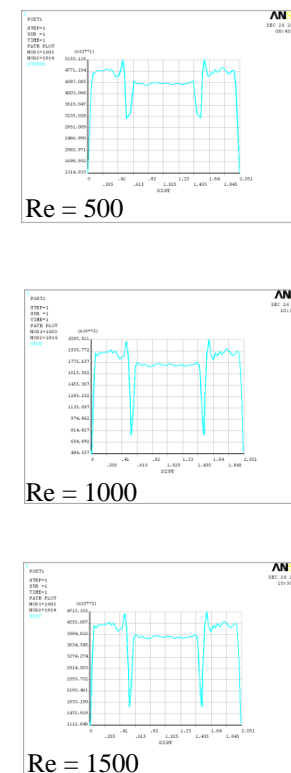


Fig. (21) Von Mises stress distribution along the copper pipe with Rigid support.

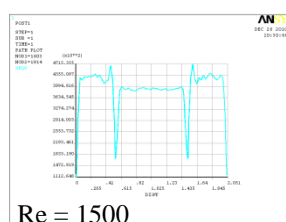
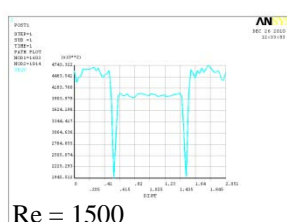
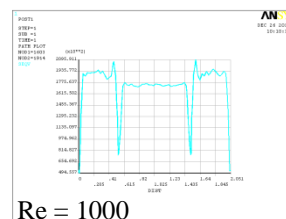
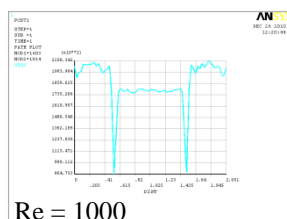
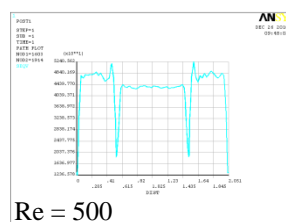
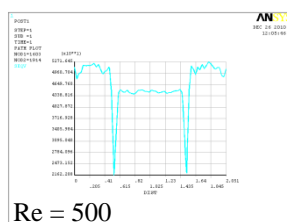


Fig. (22) Von mises stress distribution along the steel pipe with Flexible support.

Fig. (24) Von Mises stress distribution along the steel pipe with Rigid support.

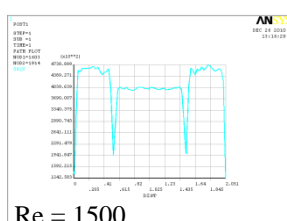
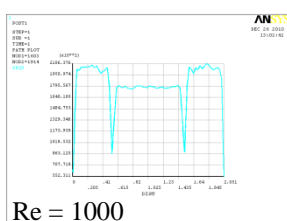
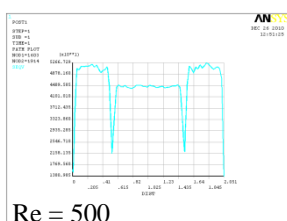


Fig. (23) Von Mises stress distribution along the steel pipe with Simply support.

Conclusions

According to the obtained results with the adopted data, the present work has reached to the following conclusions:

- Finite element method (Monolithic method) can be overcome (treated and analyzed) numerically to solve problem of fluid-structure interaction in piping system.
- The values of the natural frequencies for flexible support are less than those for simply and rigid supports. This is because the flexible support has the ability to move in y-direction. Therefore, its flexibility is very high comparing with both simply and rigid supports.
- The values of the natural frequencies for simply support are less than that for rigid support.
- The natural frequencies value in steel pipe are more than that the natural frequencies value in copper pipe. This is because of the modulus of rigidity is high in steel pipe (80-100

- GN/m²), but for copper pipe the modulus of rigidity is (30-50 GN/m²) which is given more flexibility.
- v. The values of fluid pressure force are increased with increase Reynold numbers. This is because of increased inertia force of fluid flow.
 - vi. Velocity distribution of fluid flow in piping system is clearly to be fully developed flow (the velocity cannot vary with axial direction).
 - vii. Von mises stress increased with increase Reynold numbers. This is because of inertia force of fluid flow increased which lead to increase fluid pressure.
 - viii. The loss of head due to sudden enlargement and sudden contraction is reduced the stress .

References

- 1- Nomura T. and Hughes T. J., "An Arbitrary Lagrangian-Eulerian Finite Element Method for Interaction of Fluid and a Rigid Body", *Computer Methods in Applied Mechanicals and Engineering*, vol. 95, 1992, pp. 115-138.
- 2- Childs J. S., "The Energetic Implications of Using Deforming Reference Descriptions to Simulate the Motion of Incompressible Newtonian Fluids", *Computer Methods in Applied Mechanics and Eng.*, vol. 180, 1999, pp. 219-238.
- 3- Amabili M., Pellicano F. and Paidoussis M.P., " Non-Linear Dynamics and Stability of Circular Cylindrical Shells Containing Flowing Fluid, Part I: Stability ", *Journal of Sound and Vibration*, vol. 225, 1999, pp. 655-699.
- 4- Manabe T., Tosaka N. and Honama T., " Dynamic Stability Analysis of Flow-Conveying Pipe With Two Lumped Masses By Domain Decomposition Beam ", *Fuji Research Institute Corp.*, Tokyo, Japan, 1999.
- 5- Amabili M., Pellicano F. and Paidoussis M.P, " Non-Linear Dynamics and Stability of Circular Cylindrical Shells Containing Flowing Fluid, Part IV: Large-Amplitude Vibrations With Flow ", *Journal of Sound and Vibration*, vol. 237, 2000, pp. 641-666.
- 6- Yih-Hwang Lin and Chih-Liang Chu, " Active Modal Control of Timoshenko Pipes Conveying Fluid ", *Journal of the Chinese Institute of Engineers*, vol.24, No.1, 2001, pp. 65-74.
- 7- Nawaf M. Bou-Rabee, "Numerical Stability Analysis of A Tubular Cantilevered Conveying Fluid ", *California Institute of Technology*, 2002.
- 8- Lee S. I. and Chung J., "New Non-Linear Modeling For Vibration Analysis Of A Straight Pipe Conveying Fluid ", *Journal of Sound and Vibration*, Vol. 254, 2002, pp. 313-325.
- 9- Kuiper G. L. and Metrikine A.V., "On Stability of A Clamped-Pinned Pipe Conveying Fluid ", *Heron*, Vol. 49, No.3, 2004, pp. 211-231.
- 10- Langre E., Paidoussis M. P., Doare O. and Modarres – Sadeghi Y., " Flutter of Long Flexible Cylinders In Axial Flow", *J. Fluid Mechanics*, October, 2005.
- 11- Reddy J. N., "Energy Principles and Variational Methods in Applied Mechanics", *John Wiley*, New York, 2002.
- 12- Stangl M., Gerstmayr J., and Irschik H., "A Large Deformation Finite Element for Pipes Conveying Fluid Based on The Absolute Nodal Coordinate Formulation", *ASME International Design Engineering Technical Conference and Computers*, Las Vegas, Vol. 5, 2007, pp. 1663-1672.
- 13- Jeong W. B., Seo Y. S., Jeong H. J., Lee S. H., and Yoo, W. S., "Stability Analysis of a Pipe Conveying Periodically Pulsating Fluid Using Finite Element Method," *JSME Int. J.*, Vol. 5, 2006, pp. 1116–1122.

- 14- Zhang Y. L., Gorman D. G., and Reese J. M., "A Finite Element Method for Modeling the Vibration of Initially Tensioned Thin-Walled Orthotropic Cylindrical Tubes Conveying Fluid", *sound and vibration journal*, vol. 1, 2001, pp. 93-112.
- 15- Reddy, J. N., *An Introduction to Nonlinear Finite Element Analysis*, Oxford University Press, Oxford, UK, 2004.
- 16- Zahid I. Al-hashimy, "A Theoretical Study Into The Vibration Characteristics of Different Cross-section Pipes With Different End Conditions", M.Sc. Thesis, Mechanical Engineering Department, University of Technology, Baghdad, Iraq, 2009. pp. 112.
- 17- Zena. K. Kadhim, "Vibrational Analysis of an Annulus Pipe Flow with Presence of Uniform Heat Flux", Ph.D. Thesis, Mechanical Engineering Department, University of Technology, Baghdad, Iraq, 2005, pp. 237.
- 18- Nabeel K. Abid Al-Sahib, Adnan N. Jameel, Osamah F. Abdulateef, "Investigation Into The Vibration Characteristics and Stability of a Welded Pipe Conveying Fluid" *Jordan Journal of Mechanical and Industrial Engineering*, vol. 4, June, 2010, pp. 378-387.
- 19- Ali M. Mahdi, "Experimental Investigation and Numerical Simulation of Fluid-Structure Interaction in Axial Fan System" M.Sc. Thesis, Mechanical Engineering Department, University of Technology, Baghdad, Iraq, 2010, pp. 132.
- 20- Rangwala, A. S. "Structural Dynamics of Turbo-Machines", New Age International (p) Ltd., 1st Edition, Delhi, India, 2009, pp. 430.
- 21- Khurmi R. S., and Gupta J. K. "A Textbook of Machine Design", Eurasia Publishing House (PVT.) Ltd., 14th Edition, India, 2009, pp. 1230.
- 22- Bansal R.K., "A Textbook Of Fluid Mechanics and Hydraulic Machines" Standard Publishers Distributors, 9th Edition, India, 2007, pp. 1093.